Conformational States of the Nuclear GTP-Binding Protein Ran and Its Complexes with the Exchange Factor RCC1 and the Effector Protein RanBP1†

Matthias Geyer,‡ Ralf Assheuer,§ Christian Klebe,§ Jürgen Kuhlmann,§ Jörg Becker,§ Alfred Wittinghofer,§ and Hans Robert Kalbitzer*,‡,||

Abteilung Biophysik, Max-Planck-Institut für medizinische Forschung, Jahnstrasse 29, 69120 Heidelberg, Germany, and Abteilung Strukturelle Biologie, Max-Planck-Institut für molekulare Physiologie, Rheinlanddamm 201, 44139 Dortmund, Germany

Received February 23, 1999; Revised Manuscript Received June 14, 1999

ABSTRACT: It has been shown before by ^{31}P NMR that Ras bound to the nonhydrolyzable GTP analogue guanosine 5′-*O*-(β,γ-imidotriphosphate) (GppNHp) exists in two conformations which are rapidly interconverting with a rate constant of 3200 s^{-1} at 30 °C [Geyer, M., et al. (1996) *Biochemistry 35*, 10308−10320]. Here we show that Ran complexed with GTP also exists in two conformational states, 1 and 2, which can be directly inferred from the occurrence of two ^{31}P NMR resonance lines for the γ-phosphate group of bound GTP. The exchange between the two states is slow on the NMR time scale with a value of <200 s^{-1} at 5 °C for the corresponding first-order rate constants. In wild-type Ran, the equilibrium constant K' between the two states is 0.7 at 278 K, is different for various mutants, and is strongly dependent on the temperature. The standard enthalpy $\Delta H°$ and the standard entropy $\Delta S°$ for the conformational transitions determined from the NMR spectra are as follows: $\Delta H° = 37$ kJ mol^{-1} and $\Delta S° = 130$ J mol^{-1} K^{-1} for wild-type Ran·GTP. In complex with the Ran-binding protein RanBP1, one of the Ran·GTP conformations (state 2) is stabilized. The interaction of Ran with the guanine nucleotide exchange factor protein RCC1 was also studied by ^{31}P NMR spectroscopy. In the presence of nucleotide, the ternary complex of Ran·nucleotide·RCC1, an intermediate in the guanine nucleotide exchange reaction, could be observed. A model for the conformational transition of Ran·GTP is proposed where the two states observed are caused by the structural flexibility of the effector loop of Ran; in solution, state 2 resembles the GTP-bound form found in the crystal structure of the Ran−RanBP complex.

The Ras-related nuclear protein Ran[1] is a member of the superfamily of Ras-related GTP-binding proteins which function as binary switches in signal transduction and transport processes. It is the major regulator of nucleocytoplasmic transport in regulating the import and export of proteins, RNA, and protein−RNA complexes across the nuclear pore complex (*1*, *2*). It cycles between the GTP-bound and GDP-bound state. The conversion between these two states is very slow as the dissociation of GDP from and the hydrolysis of GTP by Ran are both very slow. The Ran-bound nucleotide state is thus determined by two key regulatory proteins, the guanine nucleotide exchange factor RCC1 (*3*, *4*) and the GTPase-activating protein RanGAP (*5*, *6*). The RCC1-mediated nucleotide exchange and the RanGAP-stimulated GTP hydrolysis on Ran are both accelerated by 5 orders of magnitude (*7*, *8*). Due to the location of RCC1 in the nucleus and RanGAP in the cytoplasm, a gradient of RanGTP is established across the nuclear pore which is believed to drive nuclear transport. In the GTP-bound state, Ran interacts with two types of effector proteins, with the Ran-binding proteins such as RanBP1 (*9*) and RanBP2 (*10*, *11*) and with importin-β (*12*−*14*). Proteins of the importin-β family, all of which bind to Ran·GTP, constitute a large family of proteins involved in the actual transport of cargo in and out of the nucleus (*1*, *15*).

We have found recently by ^{31}P NMR spectroscopy (*16*) that Ras complexed with the GTP analogue GppNHp exists in two distinct conformational states, 1 and 2, which rapidly interconvert on the NMR time scale with a rate constant of 3200 s^{-1} at 30 °C. The conformational flexibility was shown to affect the switch I region. Switches I and II have been defined as the regions in Ras which change their local three-dimensional structure when going from the GDP-bound to the GTP analogue-bound form (*17*, *18*). In state 1, Tyr32 in switch I is distant from the phosphate groups of the guanosine

† This work was supported by the Deutsche Forschungsgemeinschaft, the European Community, and the Fonds der Chemischen Industrie.

* To whom correspondence should be addressed: Institut für Biophysik und Physikalische Biochemie, Universität Regensburg, Universitätsstrasse 31, D-93053 Regensburg, Germany. Telephone: +49 (0) 941/943 2594. Fax: +49 (0) 941/943 2479. E-mail: hans-robert.kalbitzer@biologie.uni-regensburg.de.

‡ Max-Planck-Institut für medizinische Forschung.

§ Max-Planck-Institut für molekulare Physiologie.

|| Present address: Universität Regensburg, Institut für Biophysik und physikalische Biochemie.

[1] Abbreviations: NMR, nuclear magnetic resonance; Ran, Ras-related nuclear protein, a product of the human Ran/TC4 gene; RCC1, protein product of the human RCC1 (regulator of chromosome condensation) gene; RanBP1, Ran-binding protein 1; Ras, protein product of the H-ras protooncogene; Raf-RBD, Ras-binding domain of the Ras effector molecule c-Raf-1; GAP, GTPase-activating protein; Rap1A, Ras proximate protein; GppNHp, guanosine 5′-*O*-(β,γ-imidotriphosphate); mantGTP, 3′-(methylanthraniloyl)-2′-deoxyguanosine diphosphate; DSS, sodium 2,2-dimethyl-2-silapentane-5-sulfonate; wt, wild-type.

10.1021/bi9904306 CCC: $18.00
Published on Web 08/12/1999

triphosphate, whereas in state 2, it is close to the phosphate groups. Binding of the Ras-binding domain of the Raf-kinase was found to stabilize state 2, whereas state 1 is involved in the interaction with GAP. The dynamic nature of the switch regions of Ras in the triphosphate-bound state was also demonstrated by proton NMR (*19*, *20*) and by EPR studies where it was suggested that Thr35 is not tightly coordinated to the γ-phosphate and the Mg^{2+} ion (*21*) as found in the crystal structure (*17*, *22*).

The three-dimensional structure of the Ran·GDP·Mg^{2+} complex has been determined by X-ray crystallography (*23*). It showed that Thr42 (corresponding to Thr35 in Ras) is far away from the nucleotide binding site and that a large conformational change has to be postulated for the Ran·GDP to Ran·GTP transition. Recently, the structure of Ran·GppNHp bound to the Ran-binding domain of RanBP2 was determined by X-ray crystallography where indeed Thr42 in switch I was found to undergo a large change between the diphosphate and the triphosphate conformation and to form the canonical interactions with both the γ-phosphate and Mg^{2+} ion exhibited by all other GTP-binding proteins (*24*). In addition, it was shown that the conformational change in the switch I region induced a large movement of the complete C-terminal extension of Ran. To determine whether the Ran−triphosphate conformation is influenced by the presence or absence of RanBP and whether conformational flexibility is a special property of Ras alone or rather an important aspect for the functioning of all Ras-related proteins, we have undertaken a NMR study of the nucleotide complexes of Ran in the absence and presence of the effector protein RanBP1. In addition, we have used ^{31}P NMR spectroscopy with Ran−nucleotide complexes and RCC1 to demonstrate the existence and investigate the properties of ternary Ran·nucleotide·RCC1 complexes which are important intermediates in the RCC1-mediated guanine nucleotide exchange on Ran.

EXPERIMENTAL PROCEDURES

Protein Expression and Preparation. Escherichia coli BL21(DE3) cells containing the expression vector pET3d-Ran (*25*) were incubated until the OD_{600} reached 0.6 at 37 °C in 5 L of standard 1-medium containing 200 μg/mL ampicillin. Protein expression was induced with 10 μM IPTG overnight at 25 °C. After incubation, the cells were washed once with PBS and stored at −80 °C. For protein preparation, the bacteria were lysed with glass beads (Ø of 0.1 mm) in lysis buffer [20 mM K_2HPO_4/KH_2PO_4, 5 mM $MgCl_2$, 6.5 mM DTE, 100 μM GDP, 1 mM PMSF, and DNase I (pH 6.4)] for 15 min on ice (4000 rpm) with the Desintegrator-S (Biomatik). After centrifugation of the crude lysate (1 h at 15 000 rpm and 4 °C), soluble proteins were purified on a 100 mL Fractogel EMD SO_3^- 650S (Merck) cation exchange column (flow rate of 2 mL/min) in Fractogel buffer [20 mM K_2HPO_4/KH_2PO_4, 5 mM $MgCl_2$, 6.5 mM DTE, and 100 μM GDP (pH 6.4)]. After washing with 200−300 mL of Fractogel buffer, Ran was eluted with a linear KCl gradient (0 to 1 M). All Ran proteins eluted between 200 and 300 mM KCl. Fractions containing Ran were concentrated and purified with Superdex G75 gel filtration (26/60 column, Pharmacia) in 50 mM K_2HPO_4/KH_2PO_4, 5 mM $MgCl_2$, 10% glycerol, and 6.5 mM DTE (pH 7.0, flow rate of 1 mL/min). Purified Ran (>95% pure, 60−150 mg) was concentrated to 10 mg/mL, shock-frozen in liquid nitrogen, and stored at −80 °C in the gel filtration buffer. All protein concentration procedures were performed with ultrafiltration methods (Amicon). The concentration of active Ran was determined as the concentration of protein-bound GDP using reverse-phase HPLC analysis on a C-18 HPLC column as described for Ras (*25*). Recombinant RCC1 (*25*) and RanBP1 (*26*) were purified as described previously.

Guanine Nucleotide Exchange. For different NMR studies, Ran-bound GDP had to be exchanged with other guanine nucleotides (GTP and GppNHp). The most efficient exchange of protein-bound GDP versus GTP was achieved with nucleotide-free Ran, although nucleotide-free Ran is fairly unstable (*7*) and up to 50% of the Ran is lost following this procedure. Recombinant Ran·GDP was incubated with alkaline phosphatase (5 units/mg Ran) in the presence of a 5-fold molar excess of $GppCH_2p$ (a gift from Roger Goody, Max-Planck-Institut, Dortmund, Germany) in 50 mM Tris, 200 mM $(NH_4)_2SO_4$, 100 nM $ZnCl_2$, and 5 mM DTE (pH 7.4) overnight at 4 °C. Completion of the digestion of GDP was monitored with HPLC analysis. After addition of phosphodiesterase (1 unit/5 mg of Ran), the reaction mixture was incubated for 3 h at room temperature. The degradation of the $GppCH_2p$ was monitored with HPLC analysis. The excess of unbound nucleotide, the hydrolysis and degradation products, and the enzymes were removed by gel filtration with a Superdex G75 column (Pharmacia, 1.6 cm × 60 cm) in 25 mM Tris, 2.5 mM $MgCl_2$, and 1 mM DTE (pH 7.4, for ^{31}P NMR measurements) or 20 mM K_2HPO_4/KH_2PO_4, 2.5 mM $MgCl_2$, and 1 mM DTE (pH 7.4, for ^1H NMR measurements). To form a 1:1 complex with GTP, nucleotide-free Ran was incubated with a 2-fold molar excess of purified GTP for 2 h on ice. Ran·GTP was purified by gel filtration with Superdex 75 as above. The concentration of Ran·GTP was measured via HPLC analysis. The exchange to Ran·GppNHp was performed with alkaline phosphatase (5 units/mg of Ran) in the presence of a 5-fold molar excess of GppNHp in 50 mM Tris, 200 mM $(NH_4)_2SO_4$, 100 nM $ZnCl_2$, and 5 mM DTE (pH 7.4) for 3 h at room temperature, similar to a procedure used for Ras (*27*). After incubation, Ran·GppNHp was purified by gel filtration with Superdex G75 and the concentration of the nucleotide-loaded Ran was measured via HPLC analysis.

Preparation of the NMR Samples. ^{31}P NMR spectra of Ran complexed with guanine nucleotides were recorded in 40 mM Tris-HCl, 5 mM $MgCl_2$, and 2 mM DTE (pH 7.4). Either 2500 μL of the sample was placed in 10 mm NMR tubes (Wilmad), or 8 mm NMR tubes (Shigemi) were used with 800 μL of the sample. The protein concentration typically varied between 0.3 and 1.2 mM. To provide a lock signal, the samples contained 10−99% D_2O. In the study of Ran complexes with RanBP1 or RCC1, usually 1 mM Ran was used and highly concentrated RanBP1 (0.8 mM) or RCC1 (0.54 mM) solutions were added. Additionally, the samples for the Ran·RCC1 concentration series were concentrated after each addition of RCC1 to avoid an excessively strong dilution of the sample and hence a decrease of the phosphorus signal.

Proton NMR experiments with Ran·GDP, Ran·GppNHp, and Ran(F35L)·GppNHp were performed using a 20 mM KP_i buffer (pH 7.2) with 5 mM $MgCl_2$ and 5 mM DTE in aqueous solution (94% H_2O/6% D_2O). For the experiments

with Ran·GDP, the protein concentration was varied from 0.4 to 2.8 mM to study aggregation effects. The ^{1}H NMR spectra of Ran triphosphate complexes were recorded with samples containing 285 μL of a 0.9 mM protein solution in 5 mm Shigemi sample tubes (Shigemi Inc.).

NMR Spectroscopy. ^{31}P NMR experiments were performed on a Bruker AMX-500 NMR spectrometer working at a phosphorus resonance frequency of 202 MHz. The ^{31}P spectra were referenced to 85% phosphoric acid contained in a glass sphere which was immersed in the sample and calibrated for various temperatures. Unless noted otherwise, phosphorus spectra were recorded at 5 °C with a total spectral width of 60 ppm. For one-dimensional ^{31}P NMR spectra, 512−16384 free induction decays were accumulated after excitation with a 65° pulse using a repetition time of 3−5 s. Most experiments were carried out in D_2O solution to avoid undesired proton phosphate couplings. A total of 32K time domain data points were recorded and transformed to 16K real data points, corresponding to a digital resolution of 0.74 Hz/point.

All spectra were processed on a Silicon Graphics Indigo2 workstation using the software packages UXNMR (Bruker, Karlsruhe, Germany) for data processing and AURELIA (*28*) for data evaluation. Phosphorus NMR spectra used for the equilibrium constant determination were filtered by an exponential window function causing no significant line broadening. Two-dimensional ^{1}H spectra were filtered by a sine-bell window multiplication function after zero-filling in the indirect dimension and Fourier transformed to 1024 × 2048 ($F_1 \times F_2$) real data points. The structure figures were produced using MOLSCRIPT (*29*).

Determination of Equilibrium Constants and Exchange Rates. The NMR spectra were evaluated with a simulation software written in the laboratory of one of the authors (H. R. Kalbitzer). The software package is written in C and runs on UNIX workstations. The simulated spectra were displayed and plotted with the program UXNMR from Bruker.

The two-site exchange for triphosphate spin systems can be described as

$$\underset{1}{\mathrm{ABC}} \underset{k_{-1}}{\overset{k_1}{\rightleftharpoons}} \underset{2}{\mathrm{A'B'C'}} \qquad (1)$$

with ABC being the α-, β-, and γ-phosphates in state 1, A′B′C′ the phosphate groups in state 2, and k_1 and k_{-1} the rate constants for the conversion between the two states. For a description of this process, the populations p_1 and p_2 of states 1 and 2 must be known. The equilibrium constant K' is given by

$$K' = k_{-1}/k_1 = p_1/p_2 \qquad (2)$$

The populations p_1 and p_2 were obtained from a line fit of the ^{31}P γ-resonance signals using an integration procedure described previously (*30*).

The temperature dependence of the equilibrium constants K' was fitted with the program Grafit (Erithacus Software Ltd.) to the equation

$$K' = \mathrm{e}^{-(\Delta H^\circ - T\Delta S^\circ)/RT} \qquad (3)$$

where R is the gas constant, T the absolute temperature, ΔH° the standard reaction enthalpy, ΔS° the standard reaction entropy.

For evaluation of the data of the Ran·GDP·RCC1 complex, the ^{31}P resonance frequencies of the ternary complex were obtained by fitting the spectrum at the lowest temperature where all three GDP forms can be observed. Here, a gradient fit procedure, using the Marquardt method (*31*), was applied to separate the six overlapping signals. The number of parameters to be fitted was reduced by using the known chemical shifts for α- and β-resonance lines of free GDP·Mg^{2+} and Ran·GDP·Mg^{2+} and by holding the relative integrals of corresponding α- and β-signals equal. The phosphorus multiplets were fitted using Lorentzian line shapes with a ^{31}P J coupling constant of 17 Hz as derived from the magnesium-bound nucleotide. Using this method, the mean half-width, the signal amplitude, and the line position of the ternary complex could be determined. From these parameters, the populations in the three different GDP complexes were derived.

An upper limit of the exchange rate τ_e^{-1} between two states in slow exchange can be estimated from the line separation $\Delta\nu$ of the two corresponding resonance lines using the slow exchange condition where $|2\pi\Delta\nu| > \tau_e^{-1}$. More accurate upper limits can be obtained assuming that the observed mean half-widths $\Delta\nu_{1/2}^1$ and $\Delta\nu_{1/2}^2$ of the resonance lines in states 1 and 2, respectively, are solely due to exchange broadening. The individual line widths $\Delta\nu_{1/2}^x$ can be approximated (*32*) by

$$\Delta\nu_{1/2}^x = 1/\pi T_2^x + 1/\pi\tau^x \qquad (4)$$

with $1/\pi T_2^x$ being the line widths of state x in the absence of exchange and τ^x the lifetimes in state 1 or 2. Assuming that the exchange broadening dominates, one obtains as an upper limit for the inverse of the lifetimes in states 1 and 2

$$1/\tau^x < \pi\Delta\nu_{1/2}^x \qquad (5)$$

RESULTS

^{31}P NMR Spectra of the Ran−Nucleotide Complexes. Phosphorus NMR spectra of the 24 kDa protein Ran complexed with GDP·Mg^{2+}, GTP·Mg^{2+}, and the nonhydrolyzable GTP analogue GppNHp·Mg^{2+} are shown in Figure 1. Since Ran has just one single high-affinity binding site for guanine nucleotides, one would expect only one resonance line for each phosphorus atom corresponding to the α-, β-, and γ-phosphate group of the bound nucleotide. The spectra of the Ran·GDP and Ran·GppNHp complexes recorded at 5 °C show the expected number of ^{31}P resonance signals with line widths corresponding to a protein with a molecular mass of 24 kDa. Surprisingly, in the Ran·GTP·Mg^{2+} complex, the γ-phosphate group splits into two lines. This indicates that the protein exists in two different conformations when GTP is bound. Integration of the individual peaks shows that the sum of the intensities of the two γ-resonance signals is equal to the α- and β-peak intensities as expected for bound trinucleotide.

A possible explanation for the observation of the two states could be that the nucleotide is complexed with magnesium in one of the states and not in the other. This is very unlikely considering the affinities of divalent ions for Ras-related

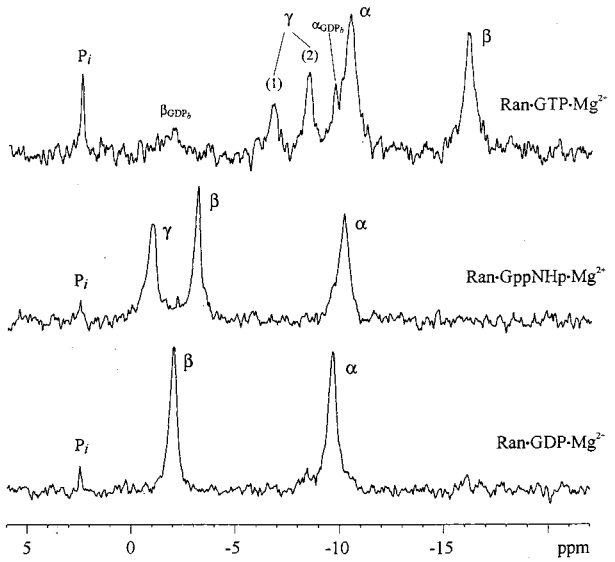

FIGURE 1: ^{31}P NMR spectra of wild-type Ran complexed with different nucleotides. Spectra were recorded at 5 °C and pH 7.4 in 40 mM Tris buffer with 5 mM Mg^{2+} in D_2O. Protein concentrations were 1.1 mM for Ran·GDP·Mg^{2+}, 0.9 mM for Ran·GppNHp·Mg^{2+}, and 0.6 mM for Ran·GTP·Mg^{2+}. Note that the number of scans accumulated varies for each spectrum.

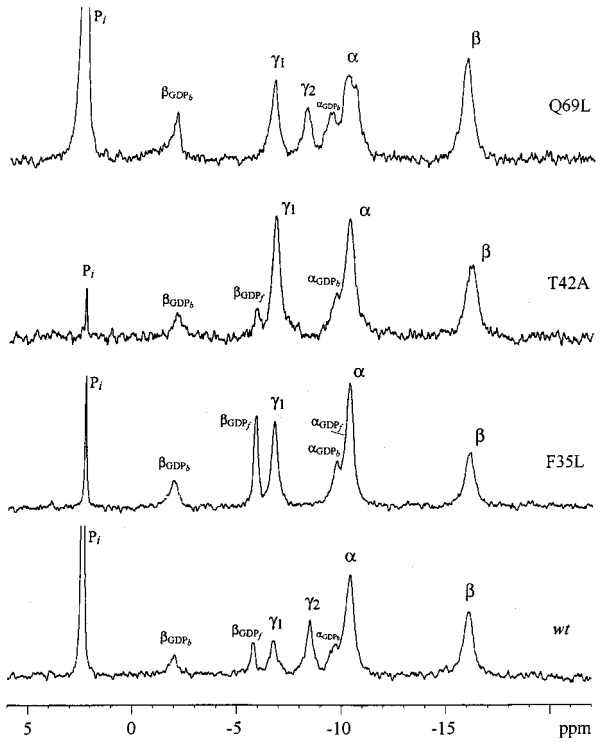

FIGURE 2: ^{31}P NMR spectra of wild-type and mutant Ran·GTP·Mg^{2+} complexes. Spectra were recorded at 5 °C and pH 7.4 in the same buffer described in the legend of Figure 1. Protein concentrations were 0.5 mM for the wild type, 0.8 mM for the F35L mutant, 0.7 mM for the T42A mutant, and 0.7 mM for the Q69L mutant, all with 5 mM free Mg^{2+}.

proteins, which are in the micromolar and 10 nM range for Ras·GDP and Ras·GppNHp, respectively (*33*), and in a similar range for Rab·GDP and Rab·GTP (*34*). Furthermore, we showed that in the range of 0.1−80 mM excess free Mg^{2+} in the NMR sample, no spectral changes were observed (data not shown). This excludes the fact that partial occupancy of the high-affinity nucleotide binding site of Ran or a possible low-affinity binding site for Mg^{2+} is responsible for the observed line splitting. Also, the line splitting and the relative populations of the two lines are not dependent on the pH value in the pH range of 6.0−9.5. The line splitting is also not an artifact of the protein preparation method since reproducible results were obtained for different protein expression and different protein purification techniques. It is also not an oligomerization or aggregation effect since in the range of 0.3−2.0 mM Ran·GTP the relative populations of the two γ-peaks do not change. In the following, we arbitrarily designate the conformational state where the γ-resonance of the nucleotide is shifted downfield relative to the other γ-position as state 1 and the state where the γ-resonance is shifted upfield as state 2 (Figure 1).

In addition, we characterized the Ran protein by ^{1}H NMR spectroscopy. The protein resonances are well-resolved with signals ranging from 11.60 to −1.94 ppm, indicating a well-defined protein structure (data not shown). Here, a concentration series with Ran·GDP concentrations from 0.3 to 2.8 mM indicates a tendency of the protein to aggregate since a significant line broadening can be observed at concentrations above 1.4 mM. To avoid aggregation effects, all the following NMR experiments were performed at concentrations of Ran of <1.1 mM.

^{31}P NMR Spectra of Mutant Ran Proteins. The structures of Ran·GDP (*23*) and of Ran·GppNHp in complex with RanBD1 from RanBP2 (*24*) have exhibited a large conformational change in the switch I region. Thus, Thr42 (corresponding to Thr35 in Ras) in Ran·GppNHp is moved to a position where it contacts the γ-phosphate and the Mg^{2+} ion. Similarly, Phe35 (Phe28) moves from a position away from the guanine base in Ran·GDP such that it is located perpendicular to the guanine base and involved in an aromatic−aromatic interaction, as determined for both Ras·GDP and Ras·GppNH/GppCH$_2$p (*17*, *22*, *35*). To investigate whether the observed conformational equilibrium is influenced by residues Phe35 and Thr42, the GTP complexes of the Ran mutants F35L and T42A were also studied. To be able to study the conformational equilibrium of Ran in the absence of GTP hydrolysis, the GTPase negative mutant Q69L (*7*) was also prepared and studied by ^{31}P NMR (Figure 2). The relative populations of the two states already described for the wild-type protein as well as the chemical shift parameters vary for each of the mutants. In the spectrum of the F35L and T42A mutants, only the γ-phosphate resonance typical of state 1 can be observed, whereas the resonance originating from state 2 is not observable. For Q69L, the resonance lines for the two states are visible again, but state 2 is less populated than in the wild-type protein.

The ^{31}P NMR spectra of wild-type Ran (Figure 1) and its mutants (data not shown) complexed with the GTP analogue GppNHp·Mg^{2+} do not exhibit a line splitting of any resonance. However, a small exchange broadening of the resonance lines of the γ-phosphate (and α-) group seems to occur, at least when compared to the β-phosphate resonance. Since the chemical shifts of the γ-phosphate resonances do not change very much in wild-type Ran·GppNHp and the three mutants (-1.03 ± 0.08 ppm) and since Ran(F35L)· and Ran(T42A)·GTP complexes apparently exist only in state 1, we assume that Ran·GppNHp·Mg^{2+} prevails in state 1. Chemical shift values and equilibrium constants derived from

Table 1: ^{31}P NMR Chemical Shifts of Different Ran·Nucleotide Complexes[a]

protein complex	chemical shift δ (ppm)[b] α	β	$\gamma(1)$	$\gamma(2)$
Ran(wt)·GDP·Mg^{2+}	−9.64	−2.01		
Ran(F35L)·GDP·Mg^{2+}	−9.74	−1.98		
Ran(T42A)·GDP·Mg^{2+}	−9.68	−2.03		
Ran(Q69L)·GDP·Mg^{2+}	−9.34	−1.97		
Ras(wt)·GDP·Mg^{2+}	−10.68	−2.03		
Ran(wt)·GppNHp·Mg^{2+}	−10.15	−3.14	−0.95	
Ran(F35L)·GppNHp·Mg^{2+}	−10.35	−3.25	−1.02	
Ran(T42A)·GppNHp·Mg^{2+}	−10.26	−3.21	−1.11	
Ran(Q69L)·GppNHp·Mg^{2+}	−10.22	−3.20	−0.98	
Ras(wt)·GppNHp·Mg^{2+}[d]	−11.15, −11.85	−2.69, −3.41	−0.41	−0.23
Ran(wt)·GTP·Mg^{2+}	−10.39	−16.02	−6.77	−8.45
Ran(F35L)·GTP·Mg^{2+}	−10.33	−16.09	−6.75	−[c]
Ran(T42A)·GTP·Mg^{2+}	−10.29	−16.11	−6.75	−[c]
Ran(Q69L)·GTP·Mg^{2+}	−10.26	−15.91	−6.66	−8.13
Ras(wt)·GTP·Mg^{2+}[d]	−11.77	−14.97	−7.99	

[a] Experimental conditions as described in the legends of Figures 1 and 2. Usually, spectra were recorded at 5 °C and pH 7.4. [b] The resonances of states 1 and 2 are designated $\gamma(1)$ and $\gamma(2)$, respectively. State 1 is defined as the state where the γ-resonance is shifted downfield relative to the second γ-resonance. [c] F35L and T42A GTP could be observed only in downfield-shifted state 1. [d] Data from ref *16*.

Table 2: Equilibrium Constants of the Two Conformational States in Ran(wt)·GTP·Mg^{2+} and Ran(Q69L)·GTP·Mg^{2+} as a Function of Temperature

protein complex	temperature (°C)	relative population of state 1:2[a] (%)	equilibrium constant K'[b]
Ran(wt)·GTP·Mg^{2+}	5	40:60	0.67
	13	50:50	1.00
	22	66:34	1.94
	30	70:30	2.33
Ran(Q69L)·GTP·Mg^{2+}	5	59:41	1.43
	15	72:28	2.57
	25	80:20	4.00

[a] The relative populations of the two conformational states were determined from the peak integrals of the ^{31}P NMR resonance lines of the γ-phosphate group in states 1 and 2. [b] The equilibrium constant K' is defined by the relative population of the two states by the equation $K' = k_{-1}/k_1 = [1]/[2]$.

the peak intensities of the individual phosphorus resonances are summarized in Tables 1 and 2.

Temperature Dependence and Thermodynamic Parameters for the Spectral Changes. Temperature variation in a conformational equilibrium usually influences exchange rate constants and/or the population of the different states and is visible in the corresponding NMR spectra as a change of line widths and line intensities, respectively. The ^{31}P NMR spectra of Ran·GTP·Mg^{2+} recorded at different temperatures show that the two γ-phosphate resonance lines remain separated in the temperature range that is studied which is typical for two conformational states in slow exchange (Figure 3). However, the line intensities of the γ-phosphate resonance lines change with temperature. This means that the relative populations of the two states shift reversibly from a higher population of state 2 at low temperatures (bottom spectrum) to a higher population of state 1 at 30 °C (second spectrum from top) and back to the initial population (top spectrum). The populations of the two states were quantified by peak integration and are listed in Table 2. The equilibrium constant (from state 1 to state 2) varies from 0.67 at 5 °C to 2.33 at 30 °C. An upper limit of the exchange rate can be obtained assuming that the observed line widths are solely due to exchange broadening (see Experimental Procedures). The mean half-widths of the phosphorus resonance lines at

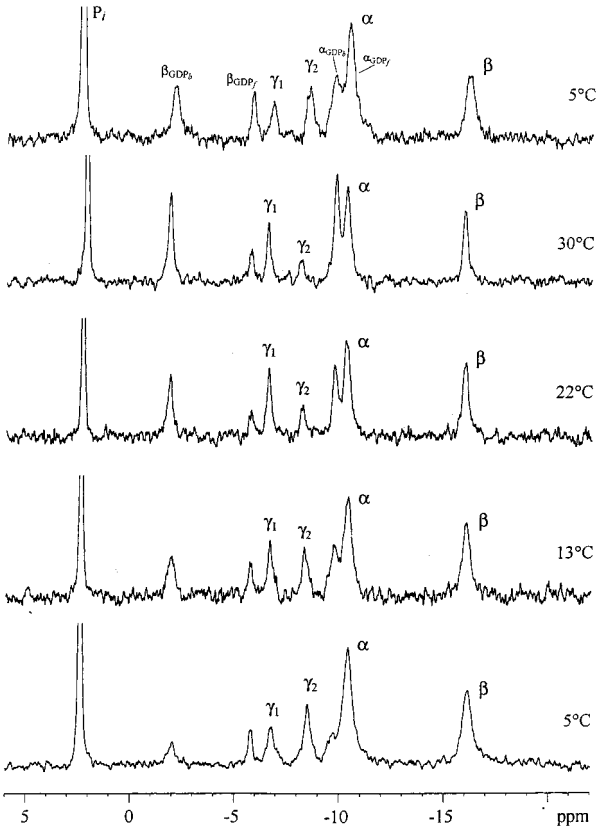

FIGURE 3: ^{31}P NMR spectra of Ran(wt)·GTP·Mg^{2+} at different temperatures. These are spectra of the same sample that was used in the experiment whose results are depicted in Figure 2. The spectra were recorded by increasing the temperature from 5 °C stepwise to 30 °C (bottom to top); the top spectrum was recorded after this temperature series.

5 °C are 103 Hz for the α-phosphate group, 105 Hz for the β-phosphate group, and 75 and 71 Hz for the γ-phosphate group in states 1 and 2, respectively. The information content of the data is not sufficient for an extensive analysis of the exchange on the basis of the density matrix theory including indirect scalar spin−spin couplings (*16*, *48*). However, if a coupling constant $^3J_{\beta\gamma}$ of 12 Hz is considered, this leads to upper limits for the rate constants k_1 and k_{-1} of 198 and 185

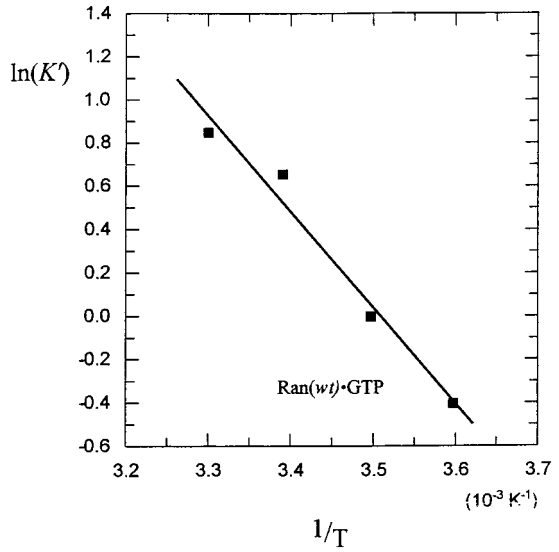

FIGURE 4: Logarithmic plot of the equilibrium constant K' of the two conformational states of Ran(wt)·GTP·Mg^{2+} vs the absolute reciprocal temperature $1/T$. The equilibrium constants derived from NMR data were fitted to eq 3 with the standard reaction enthalpy $\Delta H°$ and the standard reaction entropy $\Delta S°$ as free parameters. The values that were obtained are summerized in Table 3.

Table 3: Standard Energies for the Conformational Change in Ran(wt)·GTP·Mg^{2+} and Ran(Q69L)·GTP·Mg^{2+}[a]

	temperature (°C)	$\Delta G°$ (kJ/mol)	$\Delta H°$ (kJ/mol)	$\Delta S°$ (J/mol^{-1} K^{-1})
Ran(wt)·GTP·Mg^{2+}	5	0.9 ± 4	37.0 ± 5	130 ± 12
	20	-1.0 ± 4		
	37	-3.2 ± 4		
Ran(Q69L)·GTP·Mg^{2+}	5	-0.9 ± 4	35.3 ± 6	130 ± 17
	20	-2.8 ± 4		
	37	-5.0 ± 4		

[a] Standard free enthalpy $\Delta G°$, standard enthalpy $\Delta H°$, and standard entropy $\Delta S°$ were calculated as described in Experimental Procedures from data shown in Figure 3 and Table 2.

s^{-1}, respectively, at 5 °C (see Experimental Procedures).

We can also obtain a rough estimate of the lower limit for the exchange rate from the time needed for the adjustment of the two-state equilibrium after a temperature change. When the temperature is increased by 8 °C, the first spectra of a 0.8 mM protein sample with a sufficient signal-to-noise ratio can be observed after 15 min and be compared to a spectrum recorded later at the same temperature. Since we cannot observe a difference in the equilibrium constants determined from the two spectra, the equilibration must occur on a time scale of a few minutes, which indicates a lower limit of 10^{-3} s^{-1} for the exchange rate. The temperature-induced population changes were also recorded for the mutant Ran(Q69L)·GTP·Mg^{2+} (data not shown). The equilibrium constants derived from the NMR data are listed in Table 2.

The temperature-dependent change of the equilibrium constants can be used to calculate the standard reaction enthalpy $\Delta H°$ and the standard reaction entropy $\Delta S°$ by fitting the data to eq 3. The data obtained for wild-type Ran are presented as a logarithmic plot in Figure 4, and the obtained parameters are summarized in Table 3. As the standard enthalpy $\Delta H°$ and entropy $\Delta S°$ for wild-type Ran·GTP·Mg^{2+}, one obtains values of 37.0 ± 5 kJ/mol and 130.0 ± 12 J mol^{-1} K^{-1}, respectively. The $\Delta H°$ and $\Delta S°$ values estimated for Ran(Q69L) are 35.3 ± 6 kJ/mol and 130.0 ± 17 J mol^{-1} K^{-1}, respectively, in the same limit.

Ran·GTP in the Presence of RanBP1. As a putative effector protein of Ran, the Ran binding protein 1 (RanBP1) forms a tight complex with Ran in the triphosphate form ($K_D = 3.5$ nM at 20 °C), whereas the affinity for Ran·GDP is approximately 8000-fold weaker (*26*). Figure 5a shows the effect of increasing amounts of RanBP1 added to a solution of Ran·GTP·Mg^{2+} on the ^{31}P NMR spectra. As expected, the binding of RanBP1 causes an increase of the ^{31}P NMR resonance line width. Qualitatively, this is best visible for the β-resonance of bound GTP. However, the line width increases only by a factor 1.4 which is clearly less than 2 which is expected from binding of the 25 kDa protein RanBP1 to the 24 kDa protein Ran. This indicates that in free Ran·GTP·Mg^{2+} the β-phosphate resonance also senses the exchange between conformational states 1 and 2 and is exchange broadened. After binding to RanBP1, the exchange is suppressed and the additional exchange broadening disappears. The most striking effect of the binding of RanBP1 is the disappearance of one of the two γ-resonances of Ran. At a molar ratio of 1:1, only a single resonance line remains at the chemical shift position assigned earlier to state 2 which strongly indicates that only state 2 exists in the complex. There is also a small upfield shift of the resonance line of the β-phosphate and γ-phosphate group upon effector binding which can be best seen at molar ratios of 0.5 and 1 (Figure 5a). This shift is approximately -0.4 ppm and may be due to small side chain arrangements in the vicinity of the phosphate groups after complex formation.

Since RanBP1 seems to stabilize state 2 which becomes less populated at higher temperatures in the absence of RanBP1, we recorded the spectrum of the Ran·GTP·RanBP1 complex at different temperatures. At all the temperatures that were studied, Ran·GTP bound to RanBP1 remains in state 2 (Figure 5b). As usual, an increase in temperature leads to a line narrowing induced by the viscosity-dependent change of the rotational correlation time (Figure 5b). The chemical shifts caused by RanBP1 effector binding are summarized in Table 4. Additional information derived from the NMR spectra leads to the observation that the Ran·GTP hydrolysis rate seems not to be significantly reduced by binding to RanBP1, since the slow increase of the signals of the hydrolysis products Ran·GDP·Mg^{2+} and inorganic phosphate during the measurement time continues independent of the presence of RanBP1.

Ran·GDP Complexed with RCC1. To complete the ^{31}P NMR observation of structural changes in the GTPase cycle of Ran, we studied the effect of the addition of the exchange factor RCC1 on Ran−nucleotide complexes. A minimal scheme for the RCC1-mediated guanine nucleotide exchange reaction on Ran involving a series of binary and ternary complexes is shown in Scheme 1 (*8*).

This scheme does not include conformational changes which have to be inferred to explain the transition from tight to lose binding conformations and which might be observable by techniques such as NMR (*8*, *36*, *37*). In addition, the scheme assumes that Mg^{2+} is released together with GDP which has not been shown experimentally yet. Ternary complexes of the GTP-binding protein, nucleotide, and GEF are only very transient, and such a complex has only been

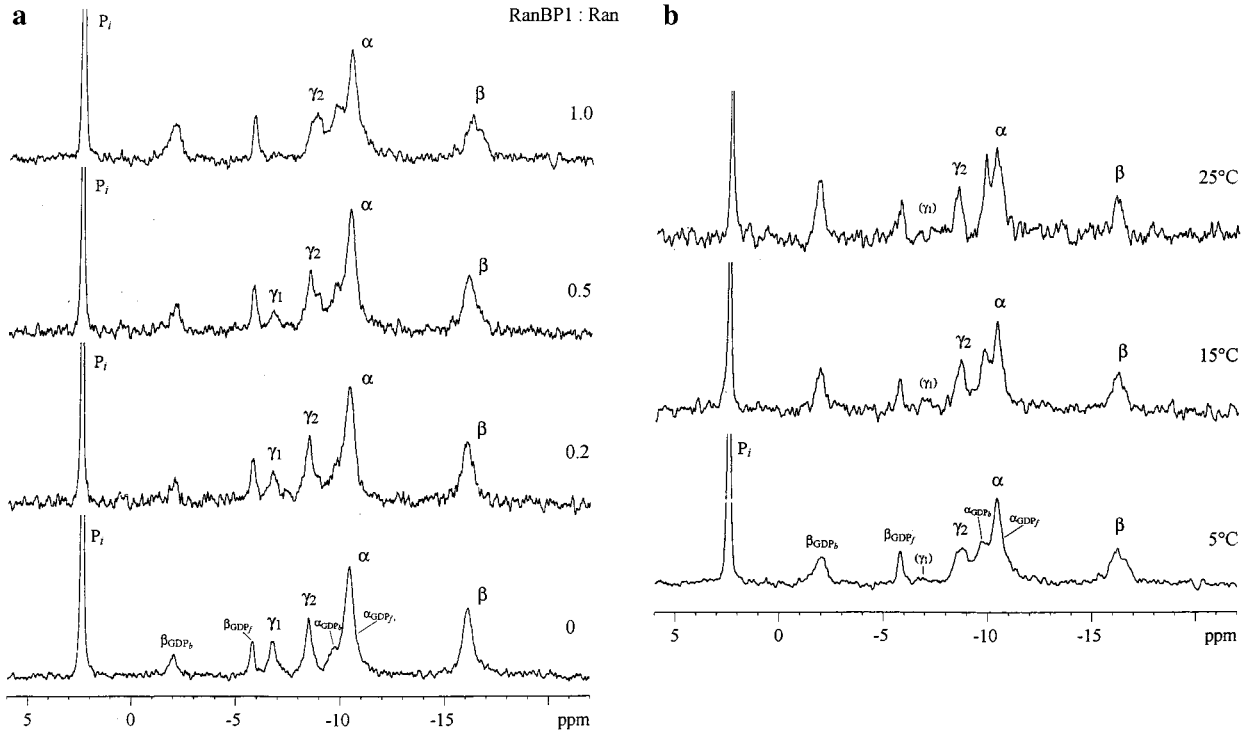

FIGURE 5: Formation of the complex of Ran·GTP·Mg^{2+} and the effector protein RanBP1. The ^{31}P NMR spectra were recorded in 40 mM Tris buffer at pH 7.4. (a) Concentration series at a temperature of 5 °C. The RanBP1 to Ran·GTP ratio varied between 0 (bottom spectrum) and 1 (top spectrum), starting with a solution of 1.1 mM Ran. (b) Temperature series of the Ran·GTP·Mg^{2+}·RanBP1 complex.

Table 4: Chemical Shifts from ^{31}P NMR Spectra of Ran Complexed with RanBP1 or RCC1 at Different Concentrations and Different Temperatures[a]

protein complex	temperature (°C)	chemical shift δ (ppm)[b] α	β	$\gamma(1)$	$\gamma(2)$
RanBP1 complexed with Ran(wt)·GTP·Mg^{2+}					
Ran(wt)·GTP·Mg^{2+}	5	−10.42	−16.10	−6.75	−8.49
Ran(wt)·GTP·Mg^{2+}·RanBP1	5	−10.40	−16.23	−	−8.70
Ran(wt)·GTP·Mg^{2+}·RanBP1	15	−10.39	−16.24	−	−8.66
Ran(wt)·GTP·Mg^{2+}·RanBP1	25	−10.28	−16.09	−	−8.50
RCC1 complexed with Ran(wt)·GDP·Mg^{2+}[c]					
GDP·Mg^{2+}		5	−10.27	−6.05	
Ran·GDP·Mg^{2+}		5	−9.45	−1.78	
Ran·GDP·(Mg^{2+})·RCC1[d]		5	−11.81	−2.51	
RCC1 complexed with Ran(Q69L)·GTP·Mg^{2+}					
Ran(Q69L)·GTP·Mg^{2+}	5	−10.35	−15.91	−6.66	−8.17
Ran(Q69L)·GTP·(Mg^{2+})·RCC1[d]	5	−10.25	−15.50	−	−8.14

[a] Experimental conditions as described in the legends of Figures 5−7. All spectra were recorded in 40 mM Tris buffer at pH 7.4. [b] The error of the chemical shift determination $\Delta\delta$ is less than ±0.1 ppm. [c] Chemical shift values as derived from the resonance line deconvolution. [d] Note that it is not known if under our conditions Mg^{2+} is bound in the active center of the complex or released after binding of RCC1.

Scheme 1

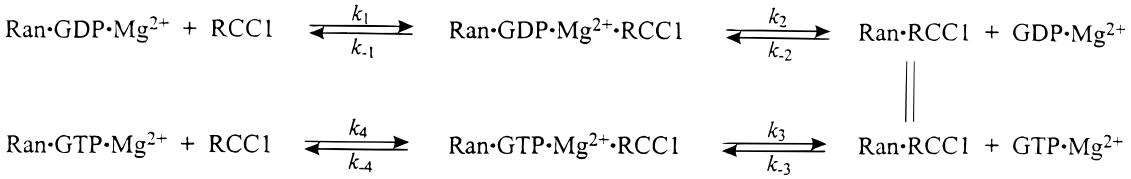

demonstrated for the Ran·RCC1·nucleotide system by fluorescence spectroscopy (*8*). When RCC1 is added in equimolar amounts to Ran·GDP (in the presence of 10 mM Mg^{2+}) at 5 °C, the ^{31}P NMR spectrum of Ran·GDP (See Figure 1) changes drastically and contains resonance lines which are not observed in the spectrum of Ran·GDP alone. They correspond to the chemical shift of free GDP and, presumably, that of the ternary Ran·GDP·RCC1 complex (Figure 6a), as summarized in Table 4. Note that no free GDP signal could be observed before addition of RCC1 and thus has to be released from Ran·GDP by RCC1. Resonance line deconvolution using the known chemical shift values for Ran·GDP·Mg^{2+} and free GDP·Mg^{2+} yields a distribution of 30% for Ran·GDP, 41% for the ternary complex Ran·GDP·RCC1, and 29% for free GDP in the reaction mixture (Figure 6b). Under our experimental conditions (10 mM free Mg^{2+}),

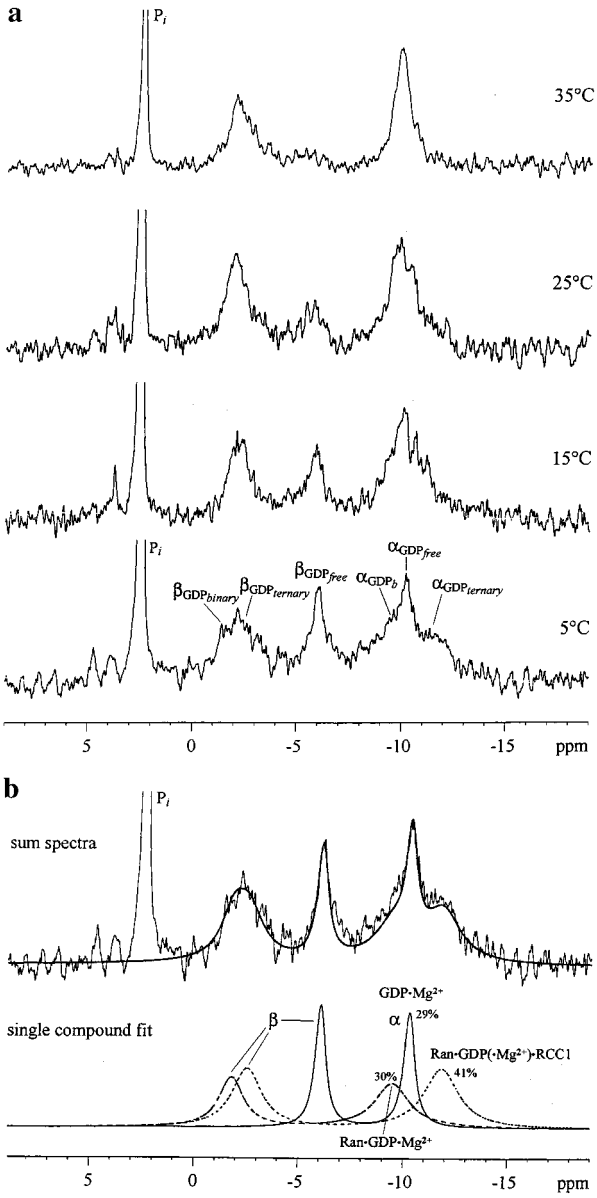

FIGURE 6: Formation of the complex of Ran(wt)·GDP·Mg^{2+} and RCC1. The ^{31}P NMR spectra of a solution of 0.65 mM Ran(wt)·GDP·Mg^{2+} and 0.66 mM RCC1 were recorded in 40 mM Tris buffer and 10 mM $MgCl_2$ at pH 7.4 in 25% D_2O/75% H_2O. (a) Temperature series from 5 (bottom spectrum) to 35 °C (top spectrum). Seven thousand to ten thousand scans were added for each spectrum. (b) Resonance line deconvolution for the 5 °C spectrum of Ran·GDP·Mg^{2+} complexed with RCC1. The whole phosphorus signal intensity of 0.65 mM GDP is distributed as follows: 29% for GDP·Mg^{2+}, 30% for Ran·GDP·Mg^{2+}, and 41% for the ternary complex of Ran·GDP·(Mg^{2+})·RCC1. Note that it is not known if under the conditions used Mg^{2+} is bound in the active center of the complex or released after binding to RCC1.

Ran·GDP and GDP should be complexed with Mg^{2+} as confirmed by the chemical shift values. However, whether the ternary Ran·GDP·RCC1 complex also contains bound Mg^{2+} is not known.

Since the total concentrations of all components in the sample are known and the relative concentrations can be derived from the integrals of the corresponding resonance lines, the relevant equilibrium constants of Scheme 1 could be estimated. However, the values depend very strongly on the accuracy of the total concentrations of the added components. Especially, possible errors in the total concentration of active RCC1 in the sample make the estimate of K_1 unreliable. Increasing the temperature to 35 °C results in the apparent disappearance of the resonance lines of Ran·GDP·Mg^{2+}·RCC1 which would mean that the equilibrium is shifted toward more than 90% Ran·GDP·Mg^{2+} or that the lines of the binary Ran·GDP·Mg^{2+} and ternary Ran·GDP·(Mg^{2+})·RCC1 coincide because of exchange averaging ($\tau_{ex}^{-1} > 3000\ s^{-1}$, calculated from the peak separation at 5 °C). Considering the high concentrations used for the experiment and the reported dissociation constants for the ternary complex, we find it unlikely that the ternary complex completely dissociates (*8*). For GDP·Mg^{2+}, the system is in slow exchange on the NMR time scale which means that at 5 °C the exchange rate (as defined in Experimental Procedures) for step 2 is less than 100 s^{-1} (as estimated from the exchange broadening); this indicates that the exchange rate increases strongly with the temperature (Figure 6).

Table 5: Intrinsic GTP Hydrolysis Rates of Ran Mutants and Binding Affinities for GST−RanBP[a]

protein	equilibrium constant K' at 25 °C[b]	hydrolysis rate k_{cat} ($\times 10^{-5}\ s^{-1}$)[c]	dissociation constant K_D (nM)[d]
Ran(wt)	2.02	5.5	3.7
Ran(F35L)	>100	1.6	492.0
Ran(T42A)	>100	1.8	651.0
Ran(Q69L)	4.01	0.3	8.2

[a] Kinetic parameters were taken from ref *47*. [b] For the wild-type protein and Ran(Q69L), the equilibrium constant K' was calculated from the fit of the data, and for F35L and T42A, the minimal peak intensity that could be detected was estimated from the signal-to-noise ratio of ^{31}P NMR spectra recorded at 25 °C. [c] The Ran·GTP hydrolysis rate was determined by HPLC analysis at 37 °C in 50 mM Tris buffer, 5 mM $MgCl_2$, and 5 mM DTE (pH 7.4). [d] The dissociation constant K_D describes the interaction between Ran·mantGppNHp and GST−RanBP1 at 25 °C.

Ran·GTP Complexed with RCC1. The hydrolysis rate of wild-type Ran·GTP is too high for recording NMR spectra with sufficient signal-to-noise ratios in the high-mass complex with RCC1. The interaction of RCC1 with Ran·GTP was therefore investigated using the Q69L mutant which exhibits the same two-state equilibrium that can be detected by two resonance lines of the γ-phosphate (Figure 2) but has a 20-fold reduced hydrolysis rate (Table 5). Figure 7 shows the ^{31}P NMR spectra of Ran(Q69L)·GTP with increasing concentrations of RCC1. Addition of 1 equiv of RCC1 leads to the release of free GTP·Mg^{2+}, which is analogous to the GDP release by RCC1 observed for Ran·GDP. Simultaneously, the β-phosphate line of protein-bound GTP, representing the binary and ternary complexes, is inhomogeneously broadened and the γ-phosphate line associated with state 1 disappears (Table 4). A further increase in the relative concentration of RCC1 leads to an increase in the line width of protein-bound GTP with a simultaneous increase in the concentration of free GTP. The line width of the β-phosphate resonance increases by a factor of approximately 3, as expected for the increase in the molecular mass from 24 kDa in Ran·GTP to 69 kDa after binding of RCC1. The position of the β-phosphate resonance of bound GTP is shifted only slightly downfield after complexation with the exchange factor (Table 4). The same seems to be true for the α-phosphate line. The γ-phosphate resonances exhibit a different behavior; the line corresponding to state 1 disappears, and the line corresponding to state 2 remains

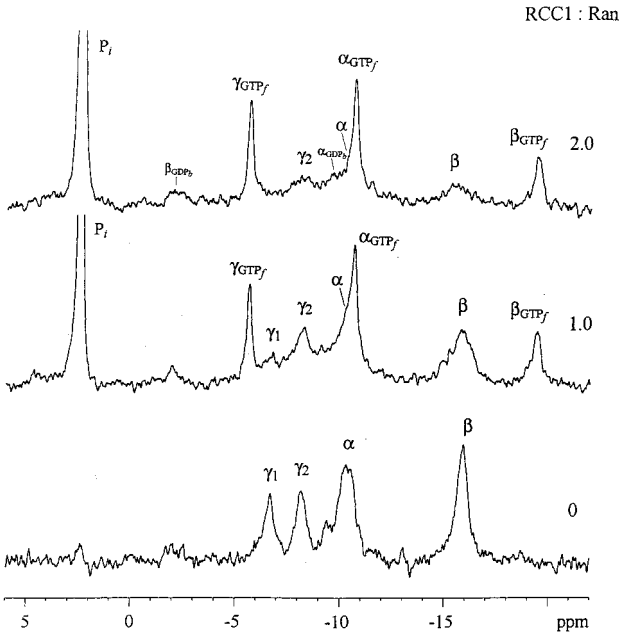

FIGURE 7: Formation of the complex of Ran(Q69L)·GTP·Mg^{2+} and RCC1. Buffer conditions are as described in the legend of Figure 6, with a temperature of 5 °C. The concentration series starts with 1.1 mM Ran(Q69L)·GTP (bottom spectrum) and ends with 370 μM Ran and 740 μM RCC1 (top spectrum). Note that the absolute intensities of the spectra cannot be compared directly because of the dilution effect and the different number of scans.

visible at the same position as in the absence of RCC1.

DISCUSSION

Two Conformational States of Ran·GTP. The ^{31}P NMR data prove that Ran·GTP occurs in two conformational states which are in equilibrium in solution. Therefore, the existence of two conformational states observed in the nucleoside triphosphate complex of Ras (*16*, *19*, *20*) is not a singular phenomenon but occurs also in Ran, and could possibly be a general feature of small GTPases. There are, however, clear differences in the dynamic properties between the two proteins. In Ras, the two states can be detected only in the complex with the GTP analogue GppNHp (*16*), whereas in Ran, they are only visible in the complex with GTP itself. This means that in a subtle way the equilibrium depends on the type of nucleoside triphosphate bound to the protein.

In wild-type Ras, the two conformational states have an almost temperature-independent standard free enthalpy, the transition between the two states requires a free activation enthalpy of approximately 90 kJ mol^{-1}. In contrast, in Ran·GTP, the standard free enthalpies for the two states differ significantly and are strongly temperature-dependent. Furthermore, the rate of interconversion between the two states is slow on the NMR time scale over the whole temperature range that was studied, but is fast on the NMR time scale for Ras at higher temperatures. Unfortunately, accurate values of the exchange rates cannot be obtained for Ran by detailed line shape analysis since this requires the observation of the transition from slow to fast exchange conditions in the NMR spectra. Therefore, only upper limits for the exchange rate constants can be determined. At low temperatures, it cannot be decided if the exchange between the two states in Ran is really slower (on an absolute time scale) than in Ras since the upper limit for k_1 of 198 s^{-1} obtained for Ran·GTP·Mg^{2+} at 5 °C would still be consistent with the k_1 value of 130 s^{-1} determined for Ras·GppNHp·Mg^{2+} at the same temperature (*16*). However, the value of 3200 s^{-1} found for Ras at 30 °C would also lead to fast exchange conditions for Ran and hence only one resonance line for the two γ-phosphate resonances of Ran. Since experimentally two lines are still observed for Ran·GTP at this temperature, the exchange rate at high temperatures between the two states is clearly slower in Ran than in Ras. The upper limit of approximately 200 s^{-1} calculated from the line widths still holds for Ran, and the rate constant k_1 at this temperature is smaller by more than 1 order of magnitude.

Ran Complexed with RanBP1. A comparison of the equilibrium constants of the two conformational states in Ran·GTP and its three mutants shows that the population of state 2 is strongly correlated with the Ran−RanBP1 dissociation constant determined by biochemical methods (Table 5); a decrease in the population of state 2 in free Ran·GTP leads to weaker binding. In addition, there seems to be a weak correlation between the prevalence of state 2 and the intrinsic hydroysis rate, suggesting that state 1 has a smaller intrinsic hydrolysis capacity.

The binding of RanBP1 to Ran·GTP·Mg^{2+} leads to the disappearance of the γ-resonance of GTP arbitrarily assigned to state 1, whereas the other resonances are mainly broadened and change their initial chemical shift position only slightly. This demonstrates that the RanBDs of RanBP1 and RanBP2 have a strong preference for Ran·GTP in the state 2 conformation. This corresponds to the findings obtained with Ras and the GTP analogue GppNHp, where the effector proteins Raf-1 (*16*), RalGEF (*38*), and AF6 (*39*) also bind preferentially to one particular conformation of Ras·GppNHp. The equilibrium constants of the two conformational states in Ran·GTP and its three mutants apparently correlate with the affinity of Ran·GTP for RanBP1 (Table 5), which further confirms that only state 2 of Ran interacts with RanBP1. This is most striking for the F35L and T42A mutants, which are only populating state 1 and have drastically reduced affinities.

Interaction of Ran with RCC1. The interaction of the exchange factor RCC1 with Ran·GDP·Mg^{2+} or Ran·GTP·Mg^{2+} leads to a partial release of the nucleotides from Ran. In addition, the ternary complex Ran·nucleotide·RCC1 can be directly observed by ^{31}P NMR spectroscopy and occurs in surprisingly high concentrations (Figures 6 and 7). The binding constants can be estimated directly from the integrals since the concentrations of the individual components in solution can be determined in one spectrum. In the complex of RCC1 with Ran·GTP·Mg^{2+}, only the signals of state 2 are visible in the ^{31}P NMR spectra which suggests that state 2 is the preferred binding conformation for RCC1. The chemical shift changes upon formation of the ternary complex are rather small for the GTP complex and more pronounced for Ran·GDP. This suggests that the environment of the phosphate groups does not change much in the GTP complex after binding the exchange factor but changes significantly in the GDP complex. According to this interpretation, the binding of RCC1 would stabilize the GTP state compared to the GDP state. Arf1 exhibits a conformational change in the switch I region similar to that of Ran, with an extra β-sheet in the GDP-bound conformation (*40*, *41*), which disappears and adopts a Ras-like conformation in the GTP-

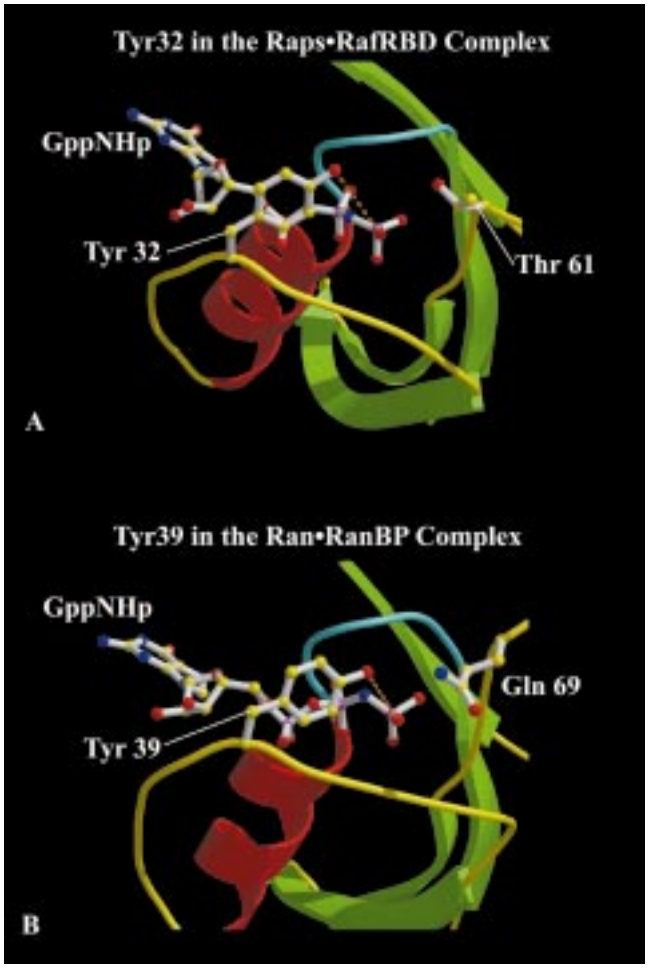

FIGURE 8: Confomational state of the effector loop of Ras·GppNHp complexed with RafRBD and Ran·GppNHp complexed with RanBD1. (A) The position of Tyr32 in the Raps·GppNHp·RafRBD complex (*43*, *44*). Raps is a mutant Rap protein that is believed to be a very close homologue of Ras (*44*). (B) The position of Tyr39 in the Ran·GppNHp·RanBP2 complex (*24*).

bound state (*42*). For the interaction between Arf and its guanine nucleotide exchange factor Gea2, it has been shown by structural studies that in the binary Arf−Gea complex, Arf adopts a more GTP-like conformation (*42*). The analogy between Arf and Ran suggests that the GTP-like conformation is an obligatory intermediate on the pathway from a binary Ran/Arf−nucleotide complex, via a ternary complex to a binary Ran/Arf−GEF complex, coming either from the Ran/Arf−GDP or the Ran/Arf−GTP direction.

Structural Basis of the Two Conformational States. The two conformational states of Ran and Ras were primarily defined by their chemical shifts, where state 2 represents the conformation in Ras·GppNHp·Mg^{2+} in which the β-phosphate resonance of bound GppNHp is shifted upfield, analogous to the upfield shift of the γ-phosphate resonance in Ran·GTP. In state 2 of Ras, Tyr32 is close to the phosphate groups which become high-field shifted by the ring current shift of the tyrosine ring. Since in the two proteins state 2 is stabilized by binding to the effectors, we can assume that they correspond to structurally similar states. In Ras, Tyr32 in the effector loop becomes coordinated to the γ-phosphate oxygen in the Rap(s)−RafRBD complex (*43*, *44*) (Figure 8A). It is conceivable that in Ran the corresponding Tyr residue (Tyr39) is also responsible for the shift. In support of this, in the structure of the Ran·GppNHp·RanBD1 complex (*24*), indeed Tyr39 shields the phosphates of GppNHp from the solvent and makes a direct contact with one of the γ-phosphate oxygens (Figure 8B), very similar to what is found for the Ras·GppNHp·RafRBD complex. One has to note that we carried out the experiments with the true substrate GTP but not with the triphosphate analogue GppNHp. However, the observation of a unique conformation in the complex in solution suggests strongly that the results obatined by X-ray crystallography with the GTP analogue can be applied also to GTP itself.

The nature of the state 2 conformation is thus most likely similar in Ras and Ran and is defined by the structure of the Ran−Ras effector complexes, whereas the conformation of Ran represented by state 1 is unclear. For Ras, it is assumed that the chemical shift difference between the two states of the β-phosphate of Ras·GppNHp is due to the flipping of the aromatic ring system of Tyr32 in a way that resembles the minor change of the Tyr32 position in the GDP, versus the GTP conformation (*17*, *18*). The conformational difference in switch I between Ran·GDP (*23*) and Ran·GppNHp in the Ran−RanBP complex is much more drastic, and resembles the conformational change seen for EF-Tu (*45*, *46*) and Arf (*40*−*42*). Thr42 of Ran (Thr35 of Ras) and Phe35 (Phe28) are far away [18 Å for Thr42 (*23*)] from the nucleotide in the GDP-bound form and become involved in the nucleotide interaction in the GppNHp form (*24*). From the effect of the ring current shift on the γ-phosphate resonance of Ran·GTP, it is clear that Tyr39 points away from the phosphate groups in state 1. This is also supported by the data from the F35A and T42A mutants which exist only in state 1 presumably because Phe35 and Thr42 are required for inducing the canonical state 2 conformation, where Phe35 is perpendicular to the base and Thr42 is involved in binding Mg^{2+} and the γ-phosphate. Whether state 1 resembles the Ran·GDP conformation is less clear, but it would mean that there is a large conformational flip-flop occurring on an intermediately fast time scale ($k_1 < 198\ s^{-1}$). It will be necessary to determine the structure of Ran·GTP or Ran·GppNHp in the absence of RanBP, possibly using the F35L or T42A mutants, as it might represent a structure more similar to the state 1 observed in the ^{31}P NMR experiments shown here.

ACKNOWLEDGMENT

We are grateful to Sabine Wohlgemuth for excellent technical assistance, Klaus Scheffzek for helpful discussions, and Kenneth C. Holmes for continuous support.

REFERENCES

1. Görlich, D. (1998) *EMBO J. 17*, 2721−2727.
2. Melchior, F., and Gerace, L. (1998) *Trends Cell Biol. 8*, 175.
3. Ohtsubo, M., Kai, R., Furuno, N., Sekiguchi, T., Sekiguchi, M., Hayashida, H., Kuma, K.-I., Miyata, T., Fukushige, S., Murotsu, T., Matsubara, K., and Nishimoto, T. (1987) *Genes Dev. 1*, 585.
4. Bischoff, F. R., and Ponstingl, H. (1991) *Nature 354*, 80−82.
5. Bischoff, F. R., Krebber, H., Kempf, T., Hermes, I., and Ponstingl, H. (1995) *Proc. Natl. Acad. Sci. U.S.A. 92*, 1749−1753.
6. Becker, J., Melchior, F., Gerke, V., Bischoff, F. R., Ponstingl, H., and Wittinghofer, A. (1995) *J. Biol. Chem. 270*, 11860−11865.

7. Klebe, C., Bischoff, F. R., Ponstingl, H., and Wittinghofer, A. (1995) *Biochemistry 34*, 639−647.
8. Klebe, C., Prinz, H., Wittinghofer, A., and Goody, R. S. (1995) *Biochemistry 34*, 12543−12552.
9. Coutavas, E., Ren, M., Openheim, J. D., D'Eustachio, P., and Rush, M. G. (1993) *Nature 366*, 585−587.
10. Yokoyama, N., Hayashi, N., Seki, T., Panté, N., Ohba, T., Nishii, K., Kuma, K., Hayashida, T., Miyata, T., Aebi, U., Fukui, M., and Nishimoto, T. (1995) *Nature 376*, 184.
11. Wu, J., Matunis, M. J., Kraemer, D., Blobel, G., and Coutavas, E. (1995) *J. Biol. Chem. 270*, 14209.
12. Floer, M., and Blobel, G. (1996) *J. Biol. Chem. 271*, 5313−5316.
13. Paschal, B. M., and Gerace, L. (1995) *J. Cell Biol. 129*, 925.
14. Görlich, D., Panté, N., Kutay, U., Aebi, U., and Bischoff, F. R. (1996) *EMBO J. 15*, 5584−5594.
15. Ullman, K. S., Powers, M. A., and Forbes, D. J. (1997) *Cell 90*, 967−970.
16. Geyer, M., Schweins, T., Herrmann, C., Prisner, T., Wittinghofer, A., and Kalbitzer, H. R. (1996) *Biochemistry 35*, 10308−10320.
17. Milburn, M. V., Tong, L., de Vos, A. M., Brünger, A., Yamaizumi, Z., Nishimura, S., and Kim, S.-H. (1990) *Science 247*, 939−945.
18. Schlichting, I., Almo, S. C., Rapp, G., Wilson, K., Petratos, K., Lentfer, A., Wittinghofer, A., Kabsch, W., Pai, E. F., Petsko, G. A., and Goody, R. S. (1990) *Nature 345*, 309−315.
19. Hu, J. S., and Redfield, A. G. (1997) *Biochemistry 36*, 5045.
20. Ito, Y., Yamasaki, K., Iwahara, J., Terada, T., Kamiya, A., Shirouzu, M., Muto, Y., Kawai, G., Yokoyama, S., Laue, E. D., Wälchli, M., Shibata, T., Nishimura, S., and Miyazawa, T. (1997) *Biochemistry 36*, 9109.
21. Halkides, C. J., Bellew, B. F., Gerfen, G. J., Farrar, C. T., Carter, P. H., Rou, B., Evans, D. A., Griffin, R. G., and Singel, D. J. (1996) *Biochemistry 35*, 12194−12200.
22. Pai, E. F., Krengel, U., Petsko, G. A., Goody, R. S., Kabsch, W., and Wittinghofer, A. (1990) *EMBO J. 9*, 2351−2359.
23. Scheffzek, K., Klebe, C., Fritz-Wolf, K., Kabsch, W., and Wittinghofer, A. (1995) *Nature 374*, 378−381.
24. Vetter, I. R., Nowak, C., Nishimoto, T., Kuhlmann, J., and Wittinghofer, A. (1999) *Nature 398*, 39−46.
25. Klebe, C., Nishimoto, T., and Wittinghofer, A. (1993) *Biochemistry 32*, 11923−11928.
26. Kuhlmann, J., Macara, I., and Wittinghofer, A. (1997) *Biochemistry 36*, 12027−12035.
27. John, J., Sohmen, R., Feuerstein, J., Linke, R., Wittinghofer, A., and Goody, R. S. (1990) *Biochemistry 29*, 6058−6065.
28. Neidig, K. P., Geyer, M., Görler, A., Antz, C., Saffrich, R., Beneicke, W., and Kalbitzer, H. R. (1995) *J. Biomol. NMR 6*, 255−270.
29. Kraulis, P. J. (1991) *J. Appl. Crystallogr. 24*, 946−950.
30. Geyer, M., Neidig, P., and Kalbitzer, H. R. (1995) *J. Magn. Reson., Ser. B 109*, 31−38.
31. Press, W. H., Flannery, B. P., Teukolsky, S. A., and Vetterling, W. T. (1986) *Numerical Recipies. The Art of Computing*, Cambridge University Press, Cambridge, U.K.
32. McLaughlin, A. C., and Leigh, J. S. (1973) *J. Magn. Reson. 9*, 296−304.
33. John, J., Rensland, H., Schlichting, I., Vetter, I., Borasio, G. D., Goody, R. S., and Wittinghofer, A. (1993) *J. Biol. Chem. 268*, 923.
34. Simon, I., Zerial, M., and Goody, R. S. (1996) *J. Biol. Chem. 271*, 20470.
35. Tong, L., de Vos, A. M., Milburn, M. V., and Kim, S.-H. (1991) *J. Mol. Biol. 217*, 503−516.
36. Wittinghofer, F. (1998) *Nature 394*, 317−320.
37. Lenzen, D., Cool, R. H., Prinz, H., Kuhlmann, J., and Wittinghofer, A. (1998) *Biochemistry 37*, 7420−7430.
38. Geyer, M., Herrmann, C., Wohlgemuth, S., Wittinghofer, A., and Kalbitzer, H. R. (1997) *Nat. Struct. Biol. 4*, 694−699.
39. Linnemann, T., Geyer, M., Jaitner, B. K., Block, C., Kalbitzer, H. R., Wittinghofer, A., and Herrmann, C. (1999) *J. Biol. Chem. 274*, 13556−13562.
40. Amor, J. C., Harrison, D. H., Kahn, R. A., and Ringe, D. (1994) *Nature 372*, 704−708.
41. Greasley, S. E., Jhoti, H., Teahan, C., Solari, R., Fensome, A., Thomas, G. M. H., Cockcroft, S., and Bax, B. (1995) *Nat. Struct. Biol. 2*, 797.
42. Goldberg, J. (1998) *Cell 95*, 237−248.
43. Nassar, N., Horn, G., Herrmann, C., Scherer, A., McCormick, F., and Wittinghofer, A. (1995) *Nature 375*, 554−560.
44. Nassar, N., Horn, G., Herrmann, C., Block, C., Janknecht, R., and Wittinghofer, A. (1996) *Nat. Struct. Biol. 3*, 723.
45. Polekhina, G., Thirup, S., Kjeldgaard, M., Nissen, P., Lippmann, C., and Nyborg, J. (1996) *Structure 4*, 1141−1151.
46. Abel, K., Yoder, M. D., Hilgenfeld, R., and Jurnak, F. (1996) *Structure 4*, 1153−1159.
47. Assheuer, R. (1997) Ph.D. Thesis, University of Bochum, Bochum, Germany.
48. Vasavada, K. V., Kaplan, J. I., and Rao, B. D. N. (1980) *J. Magn. Reson. 41*, 467−482.

BI9904306